Chapter 3
Applications of Gold Nanostars: Nanosensing, Thermal Therapy, Delivery Systems

Piersandro Pallavicini, Elisa Cabrini, Mykola Borzenkov, Laura Sironi, and Giuseppe Chirico

Abstract This chapter focuses on the most relevant applications of GNS in life science. The versatility of the GNS functionalization is combined with their optical properties to provide promising and prospective approaches in a variety of biomedical fields. Nanosensing assays, thermal treatments, and delivery systems based on GNS are discussed in this chapter.

Keywords SERS-based sensing • Hyperthermia • Photothermal effect • Smart delivery

Functionalized gold nanoparticles with controlled geometrical and optical properties are the subject of intensive studies and biomedical applications, including genomics, biosensors, immunoassays, clinical chemistry, laser phototherapy of cancer cells and tumors, and delivery platforms. In these fields targeted delivery of drugs, DNA, and antigens is coupled to optical bioimaging and the possibility to monitor cells and image details of tissues with the use of state-of-the-art detection systems [1]. Nonspherical gold nanoparticles are particularly interesting due to their capability to release locally heat with large efficiency when they are irradiated in the NIR region of the spectrum [2]. In addition their size and the shape anisotropy essentially determine the position and the amplitude of the NIR-localized surface plasmon resonance [3]. The shape of the gold nanostars (GNS), in particular, can be tuned from the shape of sea urchin to that of planar, highly regular penta-branched stars [4]. The NIR-localized surface plasmon resonance of GNS can be consequently tuned in a wide NIR range up to 1250 nm by varying the axial ratio of protruding branches and multiple LSPR band in the NIR can also be obtained [4]. The possibility to easily decorate the surface of GNS, in combination with their optical properties

P. Pallavicini • E. Cabrini
Department of Chemistry, University of Pavia, Viale Taramelli 12, Pavia 27100, Italy

M. Borzenkov (✉) • L. Sironi • G. Chirico
Department of Physics, University of Milano-Bicocca, Piazza Della Scienza 3, Milan 20216, Italy
e-mail: mykola.borzenkov@unimib.it; giuseppe.chirico@mib.infn.it

G. Chirico et al., *Gold Nanostars*, SpringerBriefs in Materials,
DOI 10.1007/978-3-319-20768-1_3

(LSPR and surface-enhanced Raman spectroscopy (SERS)), provides promising and prospective approaches of application in a variety of biomedical fields. The applications of GNS for sensing assays, thermal treatments, and target delivery are reviewed in this chapter.

3.1 Application of GNS for Sensing Assays

GNS can display tunable optical properties in the visible and NIR, which lead to strong electromagnetic field enhancement at their tips. Most of the applications of GNS for highly sensitive assays are based on the exploitation of LSPR and the correlated SERS signal. In particular, SERS provides a promising method for the detection of various biomarkers (DNA, RNA, protein, etc.) due to its high sensitivity, specificity, and capability for multiple analyte detection.

Firstly, we focus on SERS-based assays and start this review from a recently published example of the exploitation of the sensitivity of SERS-based chemical sensing [5].

In this work [5] the detection was obtained on GNS immobilized on a gold substrate via a Raman-silent organic tether. The GNS serve as the SERS substrate and facilitate the chemical sensing of analytes that can either be chemisorbed or physisorbed on the nanostars. Reported SERS substrates were capable of detecting chemisorbed 4-mercaptobenzoic acid at a concentration as low as 10 fM with a reproducible SERS enhancement factor of 10^9, and enable the semiquantitative multiplexed identification of analytes from mixtures in which they have been dissolved in variable stoichiometry. Moreover, also physisorbed analytes, such as crystal violet, could be detected with an excellent signal-to-noise ratio, hence serving as a versatile platform for the chemical identification of in principle any molecular analyte. In another more simple approach to SERS-based detection on GNS, Esenturk and Walker tested GNS for Raman enhancement using two target molecules, 2-mercaptopyridine and crystal violet [6]. They observed strong and reproducible enhancement of the Raman signal from 2-mercaptopyridine and crystal violet molecules in colloidal GNS solutions. Anisotropic, 3D nanostars produced much stronger enhanced Raman modes than nanospheres for both probe molecules. Although the Raman enhancement by nanostars and nanorods was similar for 2-mercaptopyridine at all studied concentrations of the molecule, it was significantly higher for nanostars compared to nanorods for crystal violet, in particular at low concentrations of the analyte.

A major breakthrough in online sensing was provided by Liz-Marzan et al., who immobilized GNS monolayers on transparent, flexible polydimethylsiloxane substrates, and studied their refractive index sensitivity and SERS performance [7]. They reported generalized application of GNS for ultrasensitive identification of molecules, based on both localized surface plasmon resonance and SERS. The applicability of such substrates for LSPR-based molecular sensing was demonstrated through the detection of a model analyte, mercaptoundecanoic acid. The authors further demonstrated SERS-based pesticide detection on fruit skin, by simply covering

the fruit surface at the contaminated site with the flexible plasmonic substrate. The transparency of the substrate allowed SERS detection through backside excitation, thereby facilitating practical implementation.

Gas-phase sensing could be obtained on a new SERS platform based on the deposition of ordered extended lines of poly-*N*-isopropylacrylamide (pNIPAM)-coated nanostars over large areas [8]. This system provided high and homogeneous SERS intensities, and simultaneously traps organic chemical agents as pollutants from the gas phase. pNIPAM-coated GNS were organized into parallel linear arrays. The optical properties of the fabricated substrates were investigated, and applicability for advanced sensing was demonstrated through the detection in the gas phase of pyrene traces, a well-known polyaromatic hydrocarbon.

Due to its excellent sensitivity, SERS has been capable also to achieve the single-molecule detection limit. Local pH environment has been identified to be a potential biomarker for cancer diagnosis since solid cancer is characterized by highly acidic environments [9]. An NIR SERS nanoprobe based on GNS for pH sensing was developed for future cancer detection. SERS spectrum of pH reporter under various pH environments was monitored and used for pH sensing. Furthermore, density functional theory (DFT) calculation was performed to investigate Raman spectra changes with pH at the molecular level. This study demonstrated that SERS is a sensitive tool to monitor minor molecular structural changes due to local pH environment for cancer detection.

Vo-Dinh et al. provided recently an overview of developments and applications of SERS nanosensors and nanoreporters in their laboratory for applications in biochemical monitoring, medical diagnostics, and therapy [10].

The SERS nanosensors can be used in various applications including pH sensing, protein detection, and gene diagnostics. The authors showed that GNS provide an excellent multimodality theranostic platform, combining Raman and SERS with two-photon luminescence imaging as well as photodynamic therapy, and photothermal therapy. The possibility to combine the spectral selectivity and the high sensitivity of the SERS process with the inherent molecular specificity of bioreceptor-based nanoprobes provides a unique multiplex and selective diagnostic modality. Several examples of optical detection using SERS in combination with other detection and treatment modalities are also discussed in this overview to illustrate the usefulness and potential of SERS nanosensors and nanoreporters for medical applications.

Khoury and Vo-Dinh investigated in 2008 the effect of the size of nanostars when they are used as substrates for SERS [11]. The measured SERS enhancement factors suggest an interesting correlation between the nanostar size and the SERS efficiencies, and were relatively consistent across different star samples, with the enhancement factor estimated as 5000 averaged over the 52 nm nanostars for 633 nm excitation. Solution-based SERS measurements were performed using the Raman-active dye *p*-mercaptobenzoic acid, demonstrating the use of this new nanostructure as a useful SERS-active substrate.

The Vo-Dinh research group investigated also the SERS enhancement factor (EF) of surfactant-free nanostars and applied the silica-coated SERS probe for intracellular detection [12]. The in vitro SERS detection was demonstrated by using

silica-coated SERS-encoded GNS incubated with BT549 breast cancer cells. SERS probes accumulated primarily in the cytoplasm, displaying a high SERS signal upon examination. The authors additionally confirmed that having a high EF without the need for aggregation, nanostars thus have a strong potential in sensing and imaging.

A more recent study of intracellular applications of GNS-SERS-based assay was reported by Liz-Marzan et al. These authors presented an effective method to distinguish intracellular from extracellular nanoparticles by selectively quenching the SERS signals from dye molecules adsorbed onto star-shaped gold nanoparticles that have not been internalized by cells [13]. A general method was presented to localize gold nanoparticles by means of the selective quenching of the SERS signals originating from dye-conjugated nanoparticles outside cells. This localization strategy would provide a mean for assessing the internalization efficiency of various cargos coupled with noble metal nanoparticles, such as DNA/RNA, proteins, or drugs, which are of major relevance when studying endocytosis.

Theoretical investigation of the LSPR resonances has also provided useful insights for subsequent sensing applications. Stable GNS were fabricated with tunable extinction properties from the visible spectral region up to 1800 nm, depending on the average values of core size and branch length [14]. Theoretical computations of the plasmonic properties of these nanoparticles have put into evidence the existence of hot spots located on the tips of the nanostars for wavelengths up to 1800 nm, which opens the way to the improvement of diagnostics in the IR region. Preliminary Fourier transform Raman experiments performed after functionalization with a fluorescent dye bearing end thiol groups seem to confirm the field-enhancing capability of the nanostructures at 1064 nm.

A SERS-active GNS layer on the surface of ITO glass slip has been prepared by a low-cost electrostatically assisted APTES-functionalized surface assembly method for SERS analysis [15]. It was found that the substrate assembled with the longest branches of nanostars generated the best SERS efficiency, whether the excitation source is 785 or 633 nm. The potential use of these substrates in detection applications was also investigated by using Nile blue A and rhodamine 6G. The detection limits are 5×10^{-11} M and 1×10^{-9} M, respectively, when using the 785 nm excitation source. Apart from this high enhancement effect, the substrate also showed extremely good reproducibility at the same time. The simplicity in the production of the GNS films compared to expensive lithographic methodologies, combined with the excellent reproducibility and high Raman EFs, provides an exceptionally cost-effective substrate for SERS analysis.

The first theranostic application of GNS appeared in 2013. Vo-Dinh et al. developed a non-construct that combines the possibility of Raman imaging and the photodynamic effect for medical therapy [16]. The theranostic nanoplatform was created by loading the photosensitizer, protoporphyrin IX, onto a Raman-labeled GNS. A cell-penetrating peptide, TAT, enhanced intracellular accumulation of the nanoparticles and improved their delivery and efficacy. The plasmonic GNS platform was designed to increase the Raman signal via the surface-enhanced resonance Raman scattering effect. Theranostic SERS imaging and photodynamic

therapy using this construct were demonstrated on BT-549 breast cancer cells. The TAT peptide allowed to use the GNS construct for effective Raman imaging and photosensitization after a 1-h incubation period. In the absence of the TAT peptide, nanoparticle accumulation in the cells was not sufficient to employ the Raman signal for imaging or to produce any photosensitization effect after the same incubation period.

Regarding the use of GNS-based SERS sensor of organic molecules, a simple, ultrasensitive, highly selective, and reagent-free aptamer-based biosensor has been developed for quantitative detection of adenosine triphosphate (ATP) using surface-enhanced Raman scattering [17]. The sensor contained a SERS probe made of gold nanostar@Raman label@SiO_2 core–shell nanoparticles in which the Raman-label (malachite green isothiocyanate, MGITC) molecules were sandwiched between a GNS core and a thin silica shell. Such a SERS probe brought enhanced signal and low background fluorescence, showed good water solubility and stability, and exhibited no sign of photobleaching. The aptamer labeled with the SERS probe was designed to hybridize with the cDNA on a gold film to form a rigid duplex DNA. In the presence of ATP, the interaction between ATP and the aptamer resulted in the dissociation of the duplex DNA structure and thereby removal of the SERS probe from the gold film, reducing the Raman signal. The response of the SERS biosensor varies linearly with the logarithmic ATP concentration up to 2.0 nM with a limit of detection of 12.4 pM.

Sensing of bio-molecules in biopsies was also reported by means of GNS-enhanced SERS spectroscopy. Schutz et al. presented biocompatible GNS stabilized with ethylene glycol-modified Raman reporter molecules [18]. The localization of the tumor suppressor p63 was obtained in prostate biopsies after immuno-staining with the SERS labels for optical microscopy.

Hybrid nanoparticles composed of gold and silver or iron oxide have been developed and applied to bio-sensing. Star-shaped hybrid nanoparticles have been obtained by growing a star-shaped gold coating onto a magnetic core and have been tested for biodetection via magnetic separation and via SERS [19]. A capping agent terminated with a nickel-nitrilotriacetate group showing high affinity to histidine was used to modify the surface of nanoparticles. The resulting star-shaped construct nanoparticles were used to selectively capture histidine-tagged maltose-binding protein from a crude cell extract. The performance of star-shaped nanoparticles as SERS platforms was instead demonstrated through the detection of the Raman-active dye Astra Blue.

Always in the field of hybrid gold nanoconstructs, we cite the fabrication of ultrasensitive SERS substrates based on high-density GNS assemblies on silver films with tailored surface plasmons. On these substrates multiple field enhancements from particle-film and interparticle plasmon couplings are expected and lightening rod effected of sharp tips of nanostars contributes to the enormous values of the Raman enhancement that has been described [20]. The authors showed that the interparticle and particle-film plasmon couplings of high-density GNS on metal and dielectric films can be tuned through the interparticle separation to provide maximum SERS effects. The authors observed also that the SERS enhancement factor of

GNS on a metal film as a function of interparticle separation followed a broken power law function, where the EF increases with the interparticle separation for the strong interparticle coupling range below an interparticle separation ≈0.8 times the GNS size, but decreased for the weak interparticle coupling range (for an interparticle separation of >0.8 times the GNS size). Finally, the use of tailored plasmonic substrates as ultrasensitive SERS chemical sensors with an attomole level of detection capability of 2,4-dinitrotoluene, a model compound of nitroaromatic explosives, was demonstrated.

We move now to sensors purely based on LSPR. In these constructs we can single out strong and weak coupling regions.

In general LSPR-based sensing provides a label-free technology for sensing. As an example, streptavidin molecules were detected upon binding to individual, biotin-modified GNS through the spectral shifts in the localized surface plasmon resonances [21]. The authors characterized this dependency at the single-nanoparticle level. Concentrations as low as 0.1 nM produced a shift of the tip-related plasmon resonances of about 2.3 nm (5.3 meV).

The exploitation of the dependence of the refractive index on the LSPR position is quite common for GNS, as it is for thin gold layers. In a paper published in 2013 a refractive index sensor based on LSPR in a plastic optical fiber (POF) was presented and experimentally tested [22]. LSPR was obtained by exploiting five-branched GNS obtained using Triton X-100 in a seed growth synthesis. As it was discussed in Chaps. 1 and 2 these GNS have the uncommon feature of three localized surface plasmon resonances. The strongest LSPRs fall in two ranges, one in the 600–900 nm range (LSPR 2) and the other one in the 1100–1600 nm range (LSPR 3), both sensible to refractive index changes. Due to the extremely strong attenuation (>10^2 dB/m) of the employed POF in the 1100–1600 nm range, only LSPR 2 can be exploited for refractive index change measurements, useful for biochemical sensing applications. Optical sensor system based on LSPR is shown in Scheme 3.1.

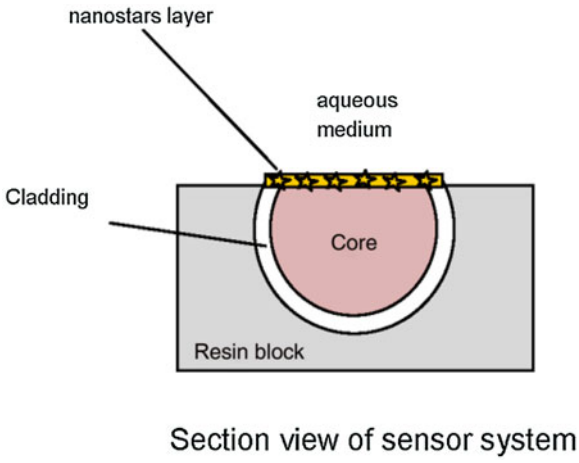

Scheme 3.1 Optical sensor system based on LSPR in POF (reproduced from Cennamo et al. [22])

The proposed device is based on the excitation of localized surface plasmons at the interface between the medium to be tested and a nanostar layer deposited on the fiber core. The sensing device has been characterized by exploiting a halogen lamp to illuminate the optical fiber and observing the transmitted spectra, normalized to the spectrum transmitted when the outer medium is air. The experimental results indicated that the configuration exhibits good performance in terms of sensitivity.

Later this method was applied for selective detection and analysis of trinitrotoluene in aqueous solution [23]. LSPR was excited in five-branched GNS, suspended in molecularly imprinted polymer specific for trinitrotoluene, which assures the selectivity. This sensing layer was deposited directly on the exposed plastic optical fiber core. The sensor showed better performance than a similar one proposed previously, in which surface plasmon resonance was excited in thin gold layer at the surface of plastic optical fiber. In the GNS sensor the sensitivity was $8.5\,10^4$ nm/M, three times higher than in the gold layer sensor. Nehl et al. described the application of single star-shaped gold nanoparticles for LSPR-based sensing [24]. The single-particle spectra demonstrated that the LSPR of single GNS are extremely sensitive to the local dielectric environment, yielding sensitivities as high as 1.41 eV photon energy shift per refractive index unit. To test their properties as molecular sensors, single-nanostar spectra were monitored upon exposure to alkanethiols and proteins known to bind gold surfaces. The observed shifts were consistent with the effects of these molecular layers on the surface plasmon resonances in continuous gold films. The obtained results suggested that LSPR sensing with single nanoparticles is analogous to the well-developed field surface plasmon resonance sensors, and would push the limits of sensitivity. The new GNS-based sensor developed at Imperial College London and the University of Vigo, Spain, can detect concentrations that are at least ten times lower than the existing ultrasensitive tests [25]. The scientists of these two groups presented a signal-generation mechanism that redefines the limit of detection of nanoparticle sensors by inducing a signal that is larger when the target molecule is less concentrated. The key step to achieve this inverse sensitivity is to use an enzyme that controls the rate of nucleation of silver nanocrystals on plasmonic transducers. The authors demonstrated the outstanding sensitivity and robustness of this approach by detecting the cancer biomarker prostate-specific antigen down to 10^{-18} g ml^{-1} (4×10^{-20} M) in whole serum.

3.2 Application of GNS for Thermal Therapy

Hyperthermia (also called thermal therapy or thermotherapy) is a type of medical treatment in which body tissue is exposed to high temperatures (up to 45–47 °C). Research has shown that high temperatures can damage and kill cancer cells, usually with minimal injury to normal tissues [26]. By killing cancer cells and damaging proteins and structures within cells, hyperthermia may shrink tumors [27]. Cells, either cancer or healthy, heated to temperatures in the range of 41–47 °C

begin to show signs of apoptosis, while by increasing temperatures above 50 °C one induces necrosis [28, 29].

Hyperthermia alone does not provide the standard of efficacy and selectivity that are required to be adopted as a cancer therapy. However, gold nanoparticles are optimal adjuvant therapies since they are known to enhance the efficacy of X-ray in tumor irradiation resulting in tumor heating and ablation [30]. Moreover, they absorb light and have been explored since long time as a method of heating [30]. For example, spherical gold nanoparticles with a peak absorption at 530 nm have been irradiated with a 514 nm laser to kill cells in vitro [31]. However, spherical GNPs absorb only visible light, so are generally poor choices for tissue heating since the penetration of UV and visible light in tissues is limited. The optimal wavelength for best tissue penetration is ~800 nm (NIR) [30]. Nonspherical gold nanoparticles are suitable prospects in this sense due to their capability to locally release heat efficiency when irradiated in NIR region where tissues are transparent [3]. It has already been mentioned that NIR plasmon resonance of GNS can be tuned in a wide NIR range up to 1250 nm [4]. Therefore, a brief overview of application of GNS for thermal treatment is made in this subchapter.

The large absorption cross sections make GNS good candidates to be used as heat sources. The presence of LSPR in NIR region reduces the flow of the impinging beam needed to heat nanoparticles, which makes more unlikely damaging of non-cancerous cells.

Rodriguez-Oliveros and Sanchez-Gil theoretically studied GNS as efficient thermal heaters at their corresponding LSPRs [32]. The authors showed that the photothermal properties of the GNS, resulting from their symmetry and geometrical dimensions, are excellent for a variety of optical heating applications. Additionally, the red shift of the LSPR induced by the increase in the number and/or sharpness of GNS tips opens the way to the use of a wide range of frequencies in the visible and near-IR regions. All their theoretical studies confirmed that GNS are promising materials for photothermal cancer application.

Nanostars, with their small core size and multiple long thin branches, exhibit high absorption cross sections that are tunable in the near-infrared region with relatively low scattering effect, making them efficient photothermal transducers [33].

The research group led by Vo-Dinh demonstrated particle tracking and photothermal ablation both in vitro and in vivo [33]. Using SKBR3 breast cancer cells incubated with bare nanostars, they observed photothermal ablation within 5 min of irradiation (980 nm continuous-wave laser, 15 W cm^{-2}). On a mouse injected systemically with PEGylated nanostars for 2 days, extravasation of nanostars was observed and localized photothermal ablation was demonstrated on a dorsal window chamber within 10 min of irradiation (785 nm continuous-wave laser, 1.1 W cm^{-2}).

Thermal therapy is also very effective in antimicrobial treatment. Regarding the specific issues of GNS in this field Pallavicini et al. grafted monolayers of GNS on mercapto-propyl-trimethoxysilane-coated glass slides [34], and showed that in these monolayers the GNS LSPR can be tuned in the 700–1100 nm range. Upon laser excitation of the NIR LSPR, an efficient photothermal response was observed, inducing local hyperthermia and efficient killing of *Staphylococcus aureus* biofilms

under laser irradiance at intensity values significantly lower than the maximum permissible exposure of skin. Chen et al. conjugated uniform GNS with cyclic RGD peptide and NIR fluorescence probe or anticancer drug (DOX) to obtain two multifunctional nanoconstructs [35]. These nanoparticles have favorable tumor-targeting capability mediated by RGD peptide binding to its overexpressed receptor on the tumor cells, both in vitro and in vivo. The multi-therapeutic analogue, Au-cRGD-DOX, integrates targeting tumor, chemotherapy, and photo-thermotherapy into a single system. The synergistic effect of photothermal therapy and chemotherapy was demonstrated in different tumor cell lines and in vivo using S180 tumor-bearing mouse models. The viability of cancer cells was only 40 % after incubation with Au-cRGD-DOX and irradiation with NIR light.

The direct monitoring of the temperature around gold nanoparticles is essential to test their therapeutic efficiency. For this reason a number of methods have been proposed [36, 37]. Regarding GNS, groups at the University of Milano-Bicocca and at the University of Pavia developed an all-optical method to measure the temperature of gold (nanorods and nanostars) and magnetite nanoparticles under NIR and radiofrequency excitation by monitoring the excited state lifetime of rhodamine B that lies ≈20 nm from the nanoparticle surface [38]. It was shown that GNS are ≈3 and ≈100 times more efficient in inducing localized hyperthermia with respect to gold nanorods and magnetite nanoparticles. The scheme of gold nanorods and GNS decorated with polyelectrolytes and temperature-sensitive dye is sketched in Scheme 3.2 together with temperature increase profile.

It is worth to mention that photothermal therapy is affected by the weakness of inducing thermotolerance in cancer cells, mediated by heat-shock proteins (HSPs) [39, 40]. These proteins have been known to play a significant role in enabling the survival of cancer cells in high-temperature conditions [40, 41]. Therefore, a synergistic approach in which photothermal therapy is combined with another therapeutic

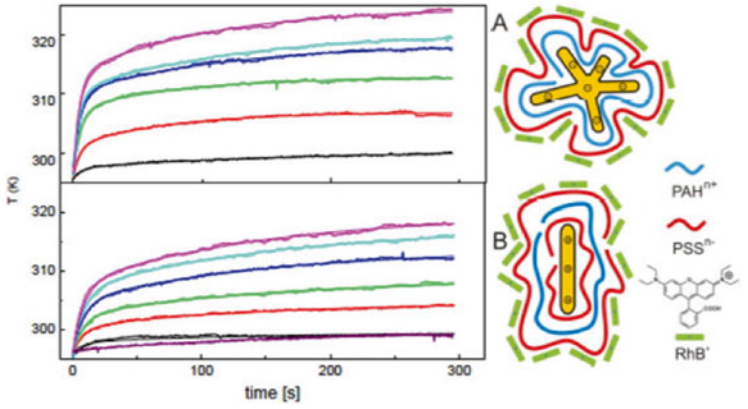

Scheme 3.2 Gold nanoparticles decorated with polyelectrolytes and dye and the temperature increase profile with polyelectrolytes and dye and the temperature increase profile under irradiation (reproduced from Freddi et al. [38])

modality is needed to overcome the limitations [40]. Chen and coworkers demonstrated that photosensitizer-coated GNS could induce a synergistic photodynamic/photothermal effect under single-laser irradiation [42].

To induce both photodynamic and photothermal effect by single NIR-CW laser, they adapted the localized surface plasmon resonance of GNS to fit the absorption of the photosensitizer chlorin e6 (Ce6). Ce6-incorporated GNS efficiently killed cancer cells in vitro upon single-laser irradiation (671 nm) compared to free Ce6-alone phototherapy.

For in vivo experiments, MDA-MB-435 tumor-bearing mouse model was intratumorally injected with the Ce6-incorporated GNS and irradiated with a single-CW laser at 4 h post-injection. The coordinated photothermal/photodynamic therapy obtained with the Ce6-incorporated GNS significantly reduced tumor growth compared to either therapeutic modality alone. It was also demonstrated in this study that synergic effect of the combined photothermal/photodynamic therapy could be modulated by adjusting the irradiation times due to photostability difference between GNS and photosensitizers.

Reduced thermotolerance can be achieved also by increasing thermal efficiency of the GNS in terms of their internalization in cells. GNS modified with a biopolymer chitosan with such improved properties were reported [43]. An in vitro photothermolysis experiment on J5 cancer cells showed that energy fluences of 23 mJ/cm^2 are necessary to cause complete death of J5 cells incubated with 4 μg/mL chitosan-capped GNS. The more uniform cellular uptake in comparison to other gold nanoparticles, like gold nanorods, allowed to use lower energy fluence for cell photothermolysis.

A stepwise fabrication of GNS-Raman reporter-photosensitizer conjugate for cancer treatment was reported in a recent paper [44]. The efficacy of such constructs as multimodal nanoprobes for SERS imaging and photodynamic/photothermal treatment of cancer was examined.

Multifunctional hybrid nanomaterials with enhanced therapeutic efficiency for externally triggered, image-guided therapy are highly attractive for nanomedicine. In a recently published paper a novel class of multifunctional hybrid nanopatches comprised of graphene oxide and GNS for enhanced photothermal effect and image-guided therapy was demonstrated [45]. The hybrid nanopatches with tunable LSPR into the NIR therapeutic window (650–900 nm) were realized using a biofriendly method that obviates the need for toxic shape-directing agents. It appears that the amphiphatic nature and the large surface area of graphene oxide enable it to serve as a soft, flexible, and biocompatible intracellular carrier for the in situ-grown plasmonic nanostructures and provide long-term biocompatibility with extremely low cytotoxicity. The photothermal transduction capabilities of graphene oxide, GNS, and graphene oxide-GNS constructs were compared. The temperature measurements of the solutions of these compounds indicated a rapid increase for the nanopatches within 2 min of laser irradiance (laser power density (0.75 W cm^{-2})) to 54.4 °C, while the same for GNS alone and for graphene oxide alone was found to be 50 and 30 °C, respectively, under the same irradiation conditions.

To monitor the therapeutic efficiency of these nanohybrids a live/dead cell assay was performed following the irradiation of the cells with 808 nm wavelength laser. As opposed to individual plasmonic nanostructures that act as nanoscale heaters, the unique nanopatch-like morphology of the hybrid construct with high density of GNS serves as a heating patch, which enhanced efficiency of local destruction of SKBR-3 cells due to their local destruction after intracellular colocalization. The perfect match of the LSPR wavelength of the GNS with the excitation of laser wavelength maximizes the photothermal effect of the nanopatch. Complete cell death occurred at ultralow laser power irradiation (0.75 W cm^{-2}) after only 2 min of laser exposure.

It should be noted that even though GNS have a remarkable photothermal transduction capability evidenced by the temperature measurements of the nanoparticle solutions, their negligible cellular uptake in the absence of surface modifications and aggregation outside the cells resulted in their poor therapeutic effect.

Jo et al. developed novel valuable therapeutic complexes, namely dual-aptamer-modified GNS, for the targeting of prostate cancers, including PSMA(+) and PSMA(−) cells [46]. The synthesized probes were subsequently analyzed for cytotoxicity tests, cell uptake, and in vitro photothermal therapy. The homogeneously well-fabricated nanostars presented high selectivity to prostate cancer cells and extremely high efficiency for therapy using an 808 nm laser under an irradiance of 0.3 W cm^{-2}, which is lower than the permitted value for skin exposure (0.329 W cm^{-2}). In another paper [47], bioconjugated GNS were tested as antigen-targeted photothermal agents for cancer treatment. GNS were biofunctionalized with nanobodies, the smallest fully functional antigen-binding fragments evolved from the variable domain, the VHH, of a camel heavy chain-only antibody [45]. These nanobodies bind to the HER2 antigen which is highly expressed on breast and ovarian cancer cells. Laser irradiation studies revealed that HER2-positive SKOV3 cells exposed to the anti-HER2-targeted GNS were destroyed after 5 min of laser treatment at 38 W cm^{-2} using a 690 nm continuous-wave laser.

3.3 GNS as Targeted Delivery Platforms

Recent advances in nanotechnology and biology are fostering the development of nanoparticles with specific functional properties that address the shortcomings of traditional disease diagnostic and therapeutic agents [48, 49]. These nanoconstructs act as excellent drug carriers (tailored drug uptake and release, low immunogenicity, etc.), offering improved efficacy for disease treatments and reduced side effects [48, 50].

The therapeutic potential of gold nanoparticles as drug-delivery carriers is primarily due to their tunable characteristics such as size, stability, and biocompatibility [51, 52]. Recently, publications from various laboratories have shown that GNS functionalized with drug molecules have a substantially increased therapeutic performance [53–56]. In these systems, drug molecules can be released from the

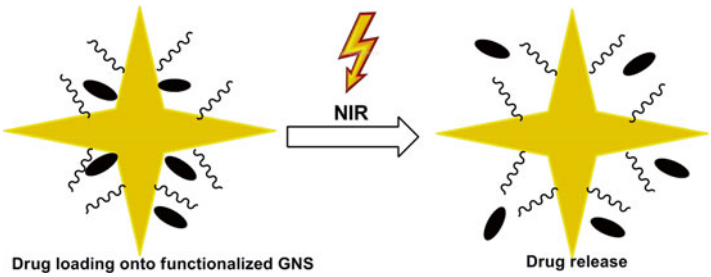

Scheme 3.3 Pictorial sketch of functionalized GNS for drug delivery

surface of GNP by desorption through ligand-exchange processes or the protonation of thiol groups at low pH [51, 57]. The increased surface volume of the star-shaped nanoparticles allows more drug to be attached and therefore potentially delivered to the target cells. However, size, shape, surface charge, and protein corona severely affect the nonspecific cellular uptake of nanoparticles, making GNS surface functionalization a key feature for the fabrication of successful delivery systems.

In this subchapter the application of GNS for targeted delivery is discussed. The schematic representation of GNS-based platforms for drug delivery is shown in Scheme 3.3.

Researchers at Northwestern University in the USA have shown that GNS can be used to carry drugs directly into the nucleus of a cancer cell [58]. This approach could be particularly useful in cases where tumors lie fairly close to the skin's surface, such as some breast cancers. In two publications Odom et al. [58, 59] studied a nanoconstruct composed of GNS loaded with the single-stranded DNA aptamer AS1411, which shows a high binding affinity for nucleolin. Nucleolin, the most abundant nucleolar phosphoprotein presents in the nuclei of normal cells, but overexpressed in the cytoplasm and plasma membranes of cancer cells [58], acts as a shuttle that carries the nanostars to the perinuclear region, where they release their drug payload. This nanoconstruct induced major changes in the nuclear phenotype through nuclear envelope invaginations near the site of the construct. Nuclear invaginations were more prominent when AS1411 aptamers were released from GNS by femtosecond laser pulses [59].

Femtosecond laser excitation of the aptamer–GNS at the localized surface plasmon resonance wavelength promoted the aptamer release by breaking its chemical bond with the gold nanoparticle. It was also shown that the release of the aptamer from the GNS at perinuclear locations not only increased the number of nuclear envelope folds but also resulted in higher apoptosis signals and cell death. This study has brought into evidence a clear correlation between drug-induced changes in nuclear phenotypes and increased therapeutic efficacy that can provide new insight into nuclear-targeted cancer therapy.

Vo-Dinh et al. demonstrated that plasmonics-active theranostic GNS can be a versatile nanoplatform for brain tumor imaging and controlled delivery of GNS into tumor in preclinical settings [60]. GNS could be delivered beyond the tumor

vasculature and deep into the tumor parenchyma. By focusing ultrafast pulsed laser irradiation through in vivo cranial window in mice preinjected with PEGylated GNS, the authors demonstrated for the first time a proof-of-concept plasmonics-enhanced optically modulated and image-guided brain tumor microvascular permeabilization and showed a highly spatial selective delivery of GNS into the tumor parenchyma with minimal off-target distribution. The authors envision a strong translational potential of plasmonics-active theranostic GNS for brain tumor molecular imaging and image-guided plasmonics-enhanced cancer therapy.

To achieve successful and selective photothermolysis, GNS need to be delivered sufficiently to the designated target cells without compromising cell viability. In general, NP size, shape, surface charge, and coating (e.g., protein corona, polymer, antifouling layer) all affect their cellular delivery. Scientists have tried numerous methods to increase the uptake of NP. One of the most efficient ways to do this is achieved by surface coating with cell-penetrating peptides (CPPs) [61].

Moreover, with a high absorption-to-scattering ratio in the NIR and multiple sharp edges favorable for heat generation, GNS efficiently transduce photon energy into heat for hyperthermia therapy. To date, most photothermolysis studies utilize laser irradiation higher than the maximal permissible exposure (MPE) of skin per ANSI regulation. Therefore, there is a strong need to design a more efficient photothermal transducer for pulsed lasers (e.g., GNS) with optimized cellular uptake.

As stressed by Vo-Dinh et al. apart from the great potential of gold nanoparticles for photothermal therapy, their intracellular delivery has to be optimized [62]. Therefore, the researchers demonstrated that TAT-peptide-functionalized GNS enter cells significantly more than bare or PEGylated GNS. The cellular uptake mechanism involves actin-driven lipid raft-mediated macropinocytosis, where particles primarily accumulate in macropinosomes and may also leak out into the cytoplasm.

Since induced angiogenesis is a major hallmark of malignant tumor, cyclic Arg-Gly-Asp (RGD) peptide-conjugated plasmonic GNS (RGD-GNS) were also prepared in order to specifically target $a_v\beta_3$ integrin overexpressed on tumor neovasculature, enabling highly sensitive angiography and photothermal therapy [63]. For the first time the authors used hemispherical photoacoustic imaging to volumetrically map the tumor angiogenesis quantitatively, offering deeper imaging depth with homogeneous resolution over existing optical imaging techniques for early diagnosis of tumor angiogenesis. This study suggests that the photoacoustic angiography with plasmonic RGD-GNS can be applied as a triple functional platform for tumor diagnosis, photothermal therapy, and treatment monitoring.

Liz-Marzan et al. in the paper published in 2014 presented seed-mediated growth of reduced graphene oxide-GNS nanocomposites and their application for anticancer drug (DOX) loading and release [64]. SERS applications of the constructs to probe DOX loading and pH-dependent release were successfully demonstrated, showing promising potential for drug delivery and chemotherapy.

Vo-Dinh et al. in 2011 reported the synthesis and characterization of surface-enhanced Raman scattering label-tagged GNS, coated with a silica shell containing methylene blue-photosensitizing drug for singlet oxygen generation [65]. To demonstrate the potential of these nanoconstructs as theranostic agents, in vitro PDT study

was performed. Methylene blue-encapsulated nanoparticles showed a significant increase in singlet oxygen generation as compared to nanoparticles synthesized without it. This increased singlet oxygen generation provided a cytotoxic effect on BT549 breast cancer cells upon laser irradiation.

Another important issue is to understand the effects that nanoparticles may have on cell function. Identifying these effects and understanding the mechanism through which nanoparticles interfere with the normal functioning of a cell are necessary for any therapeutic or diagnostic application. For this reason GNS were applied to acute mouse hippocampal slices while recording the action potentials from single neurons in the CA3 region [66]. The results showed that CA3 hippocampal neurons increase their firing rate by 17 % after the application of GNS. The increase in excitability lasted for as much as 50 min after a transient 5-min application of the nanoparticles. Further analyses of the action potential shape and computational modeling suggested that nanoparticles block potassium channels responsible for the repolarization of the action potentials, thus allowing the cell to increase its firing rate.

In this chapter the most important applications of GNS were briefly discussed. The next chapter is devoted to application of GNS as imaging agents and to the interaction of GNS with cells.

References

1. Dykman LA, Khlebstov NG (2011) Gold nanoparticles in biology and medicine: recent advances and prospects. Acta Nat 3:34–55
2. Zagar TM et al (2010) Hyperthermia combined with radiation therapy for superficial breast cancer and chest wall recurrence: a review of randomized data. Int J Hyperthermia 26:612–617
3. Huang X et al (2006) Determination of the minimum temperature required for selective photothermal destruction of cancer cells with the use of immunotargeted gold nanoparticles. Photochem Photobiol 82:412–417
4. Chirico G, Pallavicini P, Collini M (2014) Gold nanostars for superficial diseases: a promising tool for localized hyperthermia? Nanomedicine 9:1–3
5. Indrasekara ASDS et al (2014) Gold nanostars substrates for SERS-based chemical sensing in the femtomolar regime. Nanoscale 6:8891–8899
6. Esenturk NE, Walker ARH (2009) Surface-enhanced Raman scattering spectroscopy via gold nanostars. J Raman Spectrosc 40:86–91
7. Shiohara A et al (2014) Solution processed/polydimethylsiloxane/gold nanostars flexible substrates for plasmonic sensing. Nanoscale 6:9817
8. Mueller M et al (2012) Large-area organization of p-NIPAM coated nanostars as SERS platforms for polycyclic aromatic hydrocarbons sensing in gas phase. Langmuir 28:9168–9173
9. Liu Y et al (2014) Plasmonic gold nanostar for biomedical sensing. Proc SPIE 8957:895703-1
10. Vo-Dinh T et al (2015) SERS nanosensors and nanoreporters: golden opportunities in biomedical application. Wiley Interdiscip Rev Nanomed Nanobiotechnol 7:17–33
11. Khoury CG, Vo-Dinh T (2008) Gold nanostars for surface-enhanced Raman scattering: synthesis, characterization and optimization. J PhysChem C Nanometer Interfaces 112:18849–18859
12. Yuan H et al (2013) Spectral characterization and intracellular detection of surface-enhanced Raman scattering (SERS)-encoded plasmonic gold nanostars. J Raman Spectrosc 44: 234–239

13. Xie H et al (2014) Identification of intracellular gold nanoparticles using surface-enhanced Raman scattering. Nanoscale 6:12403–12407
14. Giorgetti E et al (2012) Tunable gold nanostars for surface enhanced Raman spectroscopy. Phys Stat Solidi 249:1188–1192
15. Su Q et al (2011) A reproducible SERS substrate based on electrostatically assisted APTES-functionalized surface-assembly of gold nanostars. ACS Appl Mater Interface 3:1873–1879
16. Fales AM, Yuan H, Vo-Dinh T (2013) Cell-penetrating peptide enhanced intracellular Raman imaging and photodynamic therapy. Mol Pharm 10:2291–2298
17. Li M et al (2012) Detection of adenosine triphosphate with an aptamer biosensor based on surface-enhanced Raman scattering. Anal Chem 84:2837–2842
18. Schutz M et al (2011) Hydrophilically stabilized gold nanostars as SERS labels for tissue imaging of the tumor suppressor p63 by immuno-SERS microscopy. Chem Commun 47: 4216–4218
19. Quaresma P et al (2014) Star-shaped magnetic@gold nanoparticles for protein magnetic separation and SERS detection. RSC Adv 4:3659–3667
20. Lee J (2014) Tailoring surface plasmons of high-density gold nanostars assemblies on metal films for surface-enhanced Raman spectroscopy. Nanoscale 6:616–623
21. Dondapati SK et al (2010) Label-free biosensing based on single gold nanostars as plasmonic transducers. ACS Nano 4:6318–6322
22. Cennamo N et al (2013) Localized surface plasmon resonance with five-branched gold nanostars in a plastic optical fiber for bio-chemical sensor implementation. Sensor 13: 14676–14686
23. Pesavento M et al (2014) A new approach for selective optical fiber sensor based on localized surface plasmon resonance of gold nanostars in molecularly imprinted polymer. Adv Biol Chem Eng Mater Sci 14:71–75, Proceedings of BBE '14
24. Nehl CL, Liao H, Hafner JF (2006) Plasmon resonant molecular sensing with single gold nanostars. Proc SPIE 6323:63230G–63231G
25. Rodriquez-Lorenzo L et al (2012) Plasmonic nanosensors with inverse sensitivity by means of enzyme-guided crystal growth. Nat Mater 11:604–607
26. van der Zee J (2002) Heating the patient: a promising approach? Ann Oncol 13:1173–1184
27. Hildebrandt B et al (2002) The cellular and molecular basis of hyperthermia. Crit Rev Oncol Hematol 43:33–56
28. Milleron RS, Bratton SB (2007) 'Heated' debates in apoptosis. Cell Mol Life Sci 64: 2329–2333
29. Wust P et al (2002) Hyperthermia in combined treatment of cancer. Lancet Oncol 3:487–497
30. Hainfeld JF et al (2014) Gold nanoparticle hyperthermia reduces radiotherapy doses. Nanomed Nanotechnol Biol Med 10:1609–1617
31. El-Sayed HI, Huang X, El-Sayed MA (2006) Selective laser photo-thermal therapy of epithelial carcinoma using anti-EGFR antibody conjugated gold nanoparticles. Cancer Lett 239: 129–135
32. Rodriguez-Oliveros R, Sanchez-Gil JA (2012) Gold nanostars as thermoplasmonic nanoparticles for optical heating. Opt Express 20:621–626
33. Yuan H et al (2012) In vivo particle tracking and photothermal ablation using plasmon-resonant gold nanostars. Nanomedicine 8:1355–1363
34. Pallavicini P et al (2014) Self-assembled monolayers of gold nanostars: a convenient tool for near-IR photothermal biofilm eradication. Chem Commun 50:1969–1971
35. Chen H et al (2013) Multifunctional gold nanostar conjugates for tumor imaging and combined photothermal and chemo-therapy. Theranostics 3:633–649
36. Shao J et al (2013) Photothermal nanodrugs: potential of TNF-gold nanospheres for cancer theranostics. Sci Rep. doi:10.1038/srep01293
37. Zharov V et al (2006) Photothermal nanotherapeutics for selective killing of bacteria targeted with gold nanoparticles. Biophys J 90:612–627
38. Freddi S et al (2013) A molecular thermometer for nanoparticles for optical hyperthermia. Nano Lett 13:2004–2010

39. Lepock JR (2003) Cellular effects of hyperthermia: relevance to the minimum dose for thermal damage. In J Hyperthermia 19:252–266
40. Oh J, Yoon H, Park J (2013) Nanoparticle platforms for combined photothermal and photodynamic activity. Biomed Eng Lett 3:67–73
41. Gibbons NB (2000) Heat-shock proteins inhibit induction of prostate cancer cells apoptosis. Prostate 45:58–65
42. Wang S et al (2013) Single continuous wave laser induced photodynamic/plasmonic photothermal therapy using photosensitizer-functionalized gold nanostars. Adv Mater 25:3055–3061
43. Baginskiy I et al (2013) Chitosan-modified stable colloidal gold nanostars for the thermolysis of cancer cells. J Phys Chem 117:2396–2410
44. Raghavan V et al (2014) Gold nanosensitisers for multimodal optical diagnostic imaging and therapy of cancer. J Nanomed Nanotechnol 5:6
45. Nergiz SZ et al (2014) Multifunctional hybrid nanopatches of graphene oxide and gold nanostars for ultra efficient photothermal cancer therapy. Appl Mater Interfaces. doi:10.1021/am504795d
46. Jo H et al (2014) Ultra-effective photothermal therapy for prostate cancer cells using dual aptamer-modified gold nanostars. J Mater Chem B 2:4862–4867
47. Van de Broek B et al (2011) Specific cell targeting with nanobody conjugated branched gold nanoparticles for photothermal therapy. ACS Nano 5:4319–4328
48. Veiseh O, Jonathan WG, Zhang M (2010) Design and fabrication of magnetic nanoparticles for targeted drug delivery and imaging. Adv Drug Deliv Rev 62:284–304
49. Ferrari M (2005) Cancer nanotechnology: opportunities and challenges. Nat Rev Cancer 5:161–171
50. Torchilin VP (2006) Multifunctional nanocarriers. Adv Drug Deliv Rev 58:1532–1555
51. Park C et al (2009) Ceclodextrin-covered nanoparticles for targeted delivery of an anti-cancer drug. J Mater Chem 19:2310–2315
52. Han G, Ghosh P, Rotello VM (2007) Functionalized gold nanoparticles for drug delivery. Nanomedicine 2:113–123
53. Podsiadlo P et al (2008) Gold nanoparticles enhance the anti-leukemia action of a 6-mercaptopurine chemotherapeutic agent. Langmuir 24:568–574
54. Alexander CM et al (2014) Multifunctional DNA-gold nanoparticles for targeted doxorubicin delivery. Bioconjug Chem 25:1261–1271
55. Kumar A, Zhang X, Liang X (2013) Gold nanoparticles: emerging paradigm for targeted drug delivery system. Biotechnol Adv 31:593–606
56. Li N et al (2014) Polysaccharide-gold nanocluster supramolecular conjugates as a versatile platform to the targeted delivery of anticancer drugs. Sci Rep 4, PMC3933908
57. Paciotti GF (2004) Colloidal gold: a novel nanoparticles vector for tumor directed drug delivery. Drug Deliv 11:169–183
58. Dam DH et al (2012) Direct observation of nanoparticles-cancer cell nucleus interaction. ACS Nano 6:3318–3326
59. Dam DH et al (2012) Shining light on nuclear-targeted therapy using gold nanostars constructs. Ther Deliv 3:1263–1267
60. Yuan H et al (2014) Plasmonics-enhanced and optically modulated delivery of gold nanostars into brain tumor. Nanoscale 6:4078–4082
61. Patel L, Zaro J, Shen WC (2007) Penetrating peptides: intracellular pathways and pharmaceutical perspectives. Pharm Res 24:1977–1992
62. Yuan H et al (2012) TAT-peptide functionalized gold nanostars: enhanced intracellular delivery and efficient NIR photothermal therapy using ultralow irradiance. J Am Chem Soc 134: 11358–11361
63. Nie L et al (2014) Plasmonic nanostars: in vivo volumetric photoacoustic molecular angiography and therapeutic monitoring with targeted plasmonic nanostars. Small 10:1441
64. Wang Y, Polavarapu L, Liz-Marzan L (2014) Reduced graphene oxide supported gold nanostars for improved SERS sensing and drug delivery. Appl Mater Interfaces 6:21798–21805

65. Fales AM, Yuan H, Vo-Dinh T (2011) Silica coated gold nanostars for combined SERS detection and singlet oxygen generation: a potential platform for theranostics. Langmuir 27(19):12186–12190
66. Salinas K et al (2014) Transient extracellular application of gold nanostars increases hippocampal neuronal activity. J Nanobiotechnol 14:31